Evaluation of the accuracy of the Multiple Support Response Spectrum (MSRS) method

K. Konakli
Technical University of Denmark

A. Der Kiureghian
University of California, Berkeley

SUMMARY:
The MSRS rule is a response spectrum method for analysis of multiply supported structures subjected to spatially varying ground motions. This paper evaluates the accuracy of the MSRS rule by comparing MSRS estimates of mean peak responses with corresponding "exact" mean values obtained by time-history analysis with ensembles of simulated support motions. The simulated support motions are realizations of an array of non-stationary processes with a specified coherency function, generated with a simulation approach developed elsewhere by the authors. These sets of motions are characterized by consistent variability at all support points, and thus, are appropriate as input for statistical analysis. The structural systems considered are four bridge models selected to have vastly different structural characteristics. The responses examined are pier drifts, which are quantities particularly important in performance based design of bridges. Results indicate that the MSRS method is a reliable analysis tool.

Keywords: bridges, earthquake response, ground motion spatial variability, MSRS rule, response spectrum

1. INTRODUCTION

Response spectrum methods are widely used in engineering practice for linear seismic analysis of buildings and bridges. An important advantage of the response spectrum approach over Response History Analysis (RHA) is that it provides a statistical characterization of the response, not controlled by a particular selection of ground motions. Furthermore, its simple and fast implementation is appealing from a design viewpoint and allows extended parametric analysis. For multiply supported structures subjected to spatially varying ground motions, Der Kiureghian and Neuenhofer (1992) developed the Multiple Support Response Spectrum (MSRS) method based on principles of random vibration theory. The present authors have recently generalized and extended this method to allow consideration of all response quantities and to account for the pseudo-static contributions of truncated modes (Konakli and Der Kiureghian, 2011a). The MSRS rule evaluates the mean peak response in terms of the response spectra and mean peak ground displacements at the support points of the structure, and the coherency function that characterizes the spatial variability of the support motions. The MSRS method has been used by a growing number of researchers (e.g. Loh and Ku, 1995; Kahan et al., 1996; Yu and Zhou, 2008) and has been adopted by seismic codes (Eurocode 8, 1998).

As with other response spectrum methods, the MSRS rule involves fundamental assumptions and approximations rooted in the theory of stationary random vibrations. These include the assumptions that the ground motion is a broadband process with a strong motion duration several times longer than the fundamental period of the structure and that the spatial variability of the ground motion random field is described by a smooth coherency function. The error encountered by use of MSRS is unknown and can be on either conservative or unconservative side. In this paper, errors in the MSRS estimates of the mean peak pier drifts of four bridge models are evaluated by comparisons with the respective "exact" quantities obtained from linear RHA with statistically consistent inputs. The support excitations in the RHA approach are synthetic arrays of spatially varying motions simulated with the method developed by Konakli and Der Kiureghian (2012). Comparisons between results from consistent MSRS and RHA analysis are performed for ground motion random fields characterized by different frequency contents and coherency functions.

2. STRUCTURAL RESPONSE TO SPATIALLY VARYING SUPPORT MOTIONS

Consider a lumped mass linear structural model with N unconstrained degrees of freedom (DOF) and m support DOF. Let $u_k(t)$ (k=1, ..., m) denote the prescribed support excitations. Assuming classical damping, let $s_{ki}(t)$ denote the normalized response of mode i (i=1, ..., N) to the kth support motion, obtained as the solution to

$$\ddot{s}_{ki}(t) + 2\zeta_i \omega_i \dot{s}_{ki}(t) + \omega_i^2 s_{ki}(t) = -\ddot{u}_k(t) \tag{2.1}$$

where ω_i and ζ_i respectively denote the corresponding modal frequency and damping ratio of the fixed base structure. Neglecting damping forces associated with the support DOF, a generic response quantity of interest, $z(t)$, can be expressed in terms of the support motions, $u_k(t)$, and the normalized modal responses, $s_{ki}(t)$, as follows (Der Kiureghian and Neuenhofer, 1992; Konakli and Der Kiureghian, 2011a):

$$z(t) = \sum_{k=1}^{m} a_k u_k(t) + \sum_{k=1}^{m}\sum_{i=1}^{N} b_{ki} s_{ki}(t) \tag{2.2}$$

In the preceding equation a_k represents the response quantity of interest when the kth support DOF is statically displaced by a unit amount with all other support DOF remaining fixed and b_{ki} represents the contribution of the ith mode to the response $z(t)$ arising from the excitation at the kth support DOF when $s_{ki}(t)$ is equal to unity. Coefficients a_k and b_{ki} depend only on the structural properties and can be computed by use of any conventional static analysis program (Konakli and Der Kiureghian, 2011a). The first single-sum term in Eqn. 2.2 is the pseudo-static component of the response, i.e. the static response of the system at each time instant when inertia and damping forces are ignored; this term is zero in the case of uniform support motions. The second double-sum term is the dynamic component of the response, i.e. the response of the structure to the dynamic inertia forces induced by the support motions.

Using Eqn. 2.2 and the principles of stationary random vibration theory, Der Kiureghian and Neuenhofer (1992) have shown that, for the case of translational support motions, the mean of the peak of the generic response quantity $z(t)$ can be approximately obtained in the form

$$\mathrm{E}\left[\max|z(t)|\right] \approx \left[\sum_{k=1}^{m}\sum_{l=1}^{m} a_k a_l \rho_{u_k u_l} u_{k,\max} u_{l,\max} + \sum_{k=1}^{m}\sum_{l=1}^{m}\sum_{j=1}^{N} a_k b_{lj} \rho_{u_k s_{lj}} u_{k,\max} D_l(\omega_j,\zeta_j) + \sum_{k=1}^{m}\sum_{l=1}^{m}\sum_{i=1}^{N}\sum_{j=1}^{N} b_{ki} b_{lj} \rho_{s_{ki}s_{lj}} D_k(\omega_i,\zeta_i) D_l(\omega_j,\zeta_j)\right]^{1/2} \tag{2.3}$$

The preceding equation represents the MSRS combination rule. The first, double-sum term inside the square brackets is the pseudo-static component of the response, the third, quadruple-sum term is the dynamic component, and the second, triple-sum term is a cross term of the pseudo-static and dynamic components. The mean of the peak response is given in terms of the structural properties, reflected in the coefficients a_k and b_{ki}, the mean peak ground displacements, $u_{k,\max}$, the ordinates of the mean displacement response spectrum, $D_k(\omega_i,\zeta_i)$, for each support motion and each modal frequency and damping ratio, and three sets of cross correlation coefficients: $\rho_{u_k u_l}$, describing the correlation between the kth and lth support displacements, $\rho_{u_k s_{lj}}$, describing the correlation between the kth support displacement and the response of mode j to the lth support motion, and $\rho_{s_{ki} s_{lj}}$, describing the correlation between the responses of modes i and j to the kth and lth support motions, respectively. The coefficients $\rho_{u_k u_l}$ are functions of the auto- and cross-power spectral densities (PSDs) of the support motions, whereas the coefficients $\rho_{u_k s_{lj}}$ and $\rho_{s_{ki} s_{lj}}$ additionally depend on the modal frequencies and damping ratios. The cross-PSDs of the support motions are given in terms of the corresponding auto-PSDs and the coherency function that models the spatial variability of the ground motion random field in the frequency domain. The auto-PSD of each support motion is obtained in terms of the specified response spectrum (Der Kiureghian and Neuenhofer, 1992). Thus, the set of response spectra for all support DOF (including the limits at infinite period, which equal the respective peak ground displacements) and the set of coherency functions for all pairs of support motions represent a complete specification of the input ground motions required in the MSRS analysis.

3. BRIDGE MODELS

The structural systems considered in this study are idealized models of four real bridges with vastly different structural characteristics. The bridges have been designed by the California Department of Transportation (Caltrans) and the corresponding bridge models have been developed according to Caltrans specifications (Caltrans SDC, 2004). A brief presentation of the models is provided in the following; a detailed description is given in Konakli and Der Kiureghian (2011b).

The Penstock Bridge, shown in Figure 3.1 (upper left graph), is a four-span bridge with one pier per bent and a prestressed concrete box girder. The deck has a vertical grade, varying from 0.3% to 2.1%, and a constant horizontal curvature of radius R = 458m. The columns are considered rigidly connected to the deck at the top and fixed in all directions at the bottom. The ends of the bridge are supported on seat abutments. Following Caltrans specifications, the horizontal response of the abutments is modeled through translational springs, whereas vertical translations are fully constrained. The finite element model of the bridge consists of 3 elements per pier and 6, 8, 8 and 4 elements in spans 1, 2, 3 and 4, respectively. Vertical rigid frame elements are used to connect the tops of the piers with the deck. Condensing out the rotational DOF and accounting for the constraints imposed by the rigid elements, the structure has 103 translational unconstrained DOF and 15 translational support DOF. The fundamental period of the bridge model is T = 2.38s.

The South Ingram Slough Bridge, shown in Figure 3.1 (lower left graph), is a two-span bridge with two piers per bent and a prestressed-concrete box girder. The deck has a vertical grade, varying from −0.52% to −0.85%, and a constant horizontal curvature of radius R = 1542.3m. The columns are considered rigidly connected to the deck at the top and fixed in all translational and rotational directions at the bottom. The two ends of the bridge are supported on seat abutments. The finite element model of the bridge consists of 3 elements per pier and 6 elements in each span. Vertical rigid frame elements are used to connect the tops of the piers with the deck. Condensing out the rotational DOF and accounting for the constraints imposed by the rigid elements, the structure has 55 translational unconstrained DOF and 12 translational support DOF. The fundamental period of the bridge model is T = 1.24s.

The Big Rock Wash Bridge, shown in Figure 3.1 (upper right graph), is a three-span bridge with three piers per bent and a prestressed concrete box girder. The longitudinal axis of the bridge, X, is a straight line. The deck is characterized by a constant profile grade of 0.5%. The piers are assumed to be rigidly connected to the deck at the top, whereas the bottom supports are fixed in all translational directions and free in all rotational directions. The two ends of the bridge are supported on seat abutments. The finite element model of the bridge consists of 3 elements per pier and 4 elements per span. Vertical rigid frame elements are used for the connection of the upper column elements with the girder elements. Condensing out the rotational DOF and accounting for the constraints imposed by the rigid elements, the structure is modeled with 89 translational unconstrained DOF and 24 translational support DOF. The fundamental period of the structure is $T = 0.61$s.

The Auburn Ravine Bridge, shown in Figure 3.1 (lower right graph), is a six-span bridge with two piers per bent and a prestressed-concrete box girder. The deck has a vertical grade of 0.3% and a horizontal curvature of radius $R = 1616$m. The piers are considered rigidly connected to the deck at the top, whereas the bottom supports are fixed in all translational directions and free in all rotational directions. The two ends of the bridge are supported on seat abutments. The finite element model of the bridge consists of 3 elements per pier and 4 elements per span. The top of each pier is connected with the deck through two rigid frame elements: one vertical and one in the direction of the line connecting the tops of the piers in the bent. Condensing out the rotational DOF and accounting for the constraints imposed by the rigid elements, the structure has 163 translational unconstrained DOF and 36 translational support DOF. The fundamental period of the bridge model is $T = 0.59$s.

In the RHA analysis, Rayleigh damping is assumed, with the parameters adjusted so that the damping ratios of the lower modes are close to 5%.

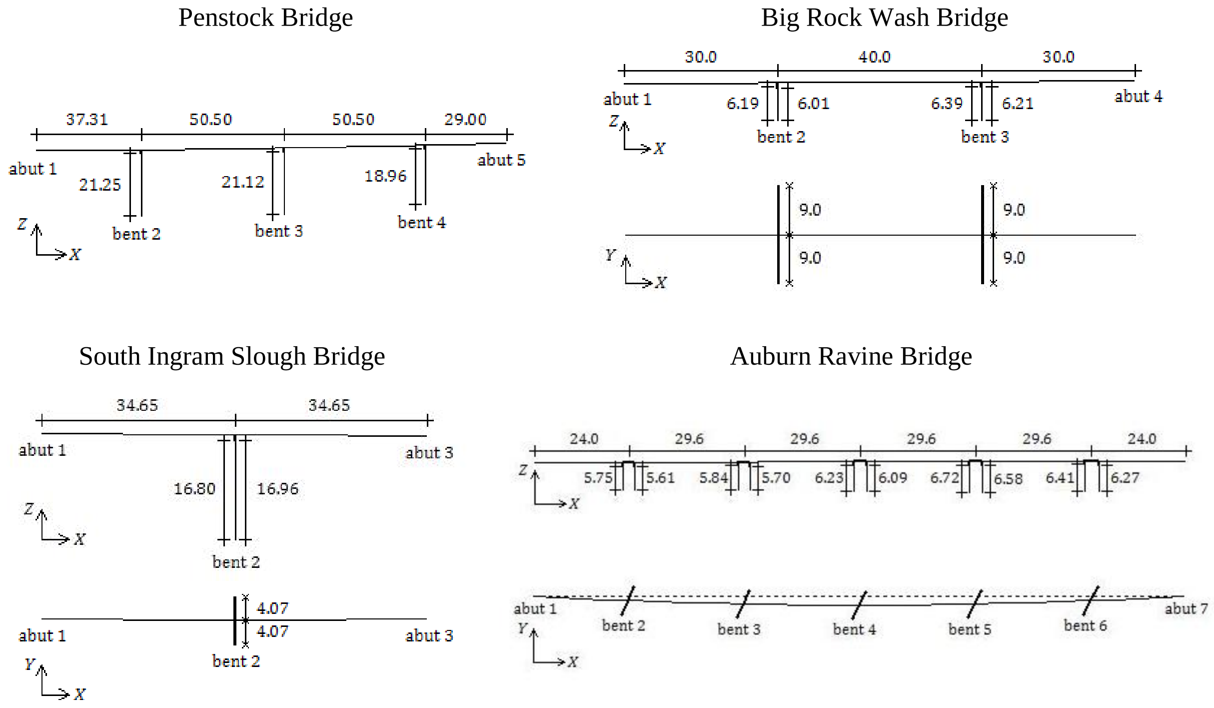

Figure 3.1. Bridge models

4. GROUND MOTION INPUT

The ground motion inputs in the RHA and MSRS analyses are consistent, i.e., the response spectra and the coherency function used to evaluate the terms in the MSRS rule represent average properties of the ensembles of support excitations used to perform RHA.

Closely spaced records of ground motions are rare; furthermore, distances between recording stations differ from the distances between support points of specific structural models to be analyzed. Thus, RHA for multiply supported structures has to rely on synthetic ground motions. In this study, the RHA input consists of synthetic arrays of motions generated using the simulation method developed in Konakli and Der Kiureghian (2012). Spatial variability of ground motion arrays simulated with this method incorporates the effects of (i) incoherence, i.e. the loss of coherency of seismic waves with distance as represented by random differences in the amplitudes and phases of the waves, (ii) wave passage, i.e. the deterministic time delay in the arrival of seismic waves at separate stations, and (iii) variation of soil conditions underneath the supports and the way it affects the amplitude and frequency content of the surface motions. For uniform soil conditions, this simulation method only requires specification of a seed accelerogram at a reference location and a coherency function that describes the spatial variability of the ground motion random field. Two approaches were developed in the aforementioned work: the conditional simulation method, which preserves time-history characteristics of the specified seed record and generates arrays of motions characterized by increasing variability with distance from the reference location; and the unconditional simulation method, which generates arrays of motions that preserve the overall temporal and spectral characteristics of the specified seed record and exhibit uniform variability at all locations. Since uniform variability is essential for consistent comparisons between the MSRS and RHA, the unconditional approach is employed in this study.

In this study, arrays of spatially varying ground motions are simulated for two seed accelerograms; the fault-normal components of the Hollister South & Pine (HSP) record from the 1989 Loma Prieta earthquake, and the fault-normal component of the Pacoima Dam (PUL) record from the 1971 San Fernando earthquake. For each record, Figures 4.1 and 4.2 show the acceleration time histories and corresponding response spectra, respectively.

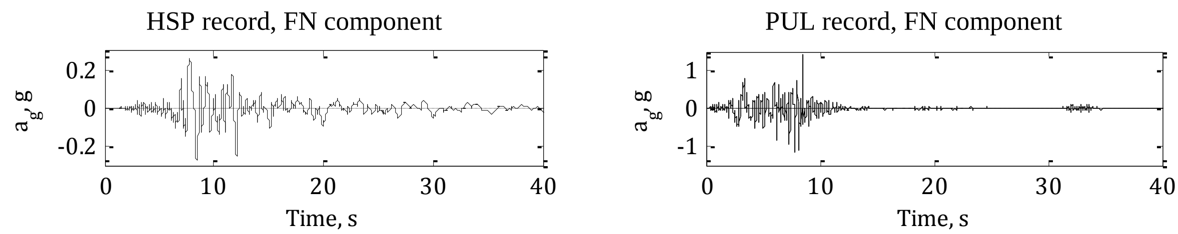

Figure 4.1. Acceleration time histories of seed records

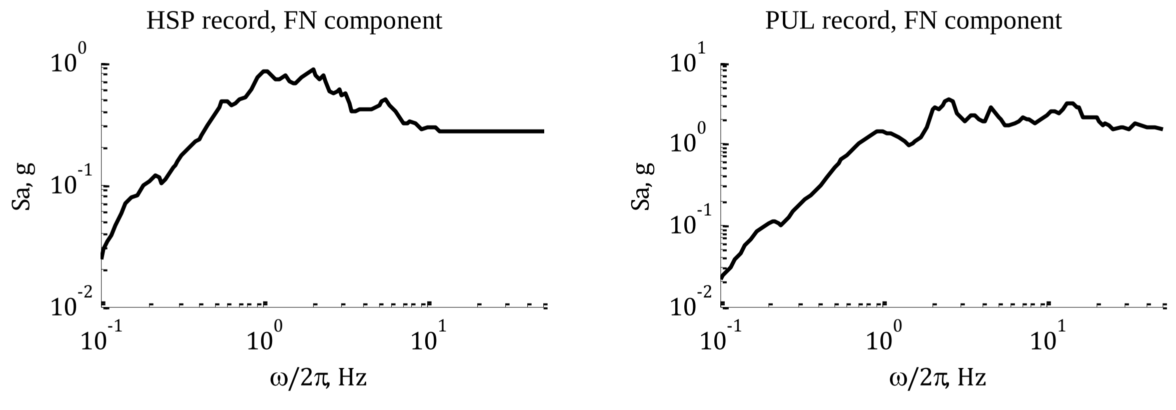

Figure 4.2. Acceleration response spectra of seed records

The coherency model employed to describe the spatial variability between the ground motion processes at two sites, *k* and *l*, is a function of the frequency, ω, and is given by

$$\gamma_{kl}(\omega) = \exp\left[-\left(a d_{kl} \omega / v_s\right)^2\right] \exp\left(i \omega d_{kl}^L / v_{app}\right) \tag{4.1}$$

where a is an incoherence parameter, d_{kl} is the distance between the sites *k* and *l*, v_s is the average shear wave velocity of the ground medium along the wave travel path, d_{kl}^L is the projected algebraic horizontal distance in the longitudinal direction of propagation of waves, and v_{app} is the surface apparent wave velocity. In this model, the modulus and phase shift of the coherency function represent the effects of incoherence and wave passage, respectively (Der Kiureghian, 1996). For the incoherence component, the model by Luco and Wong (1986) has been adopted.

For all bridges, it is assumed that the waves propagate in the direction from abutment 1 to the abutment at the other end of the bridge. The values of shear wave velocity and apparent wave velocity are taken to be $v_s = 600\text{m/s}$ and $v_{app} = 400\text{m/s}$, respectively. Analyses of recorded arrays have shown that the rate of decay of the incoherence component described by the incoherence parameter can vary significantly between different arrays (Harichandran and Vanmarcke, 1986; Abrahamson et al., 1991). Smaller values of the incoherence parameter indicate more coherent motions. To assess the effect of variations in the incoherence parameter, the values of $a = 0.2$ and $a = 0.4$ are considered when the HSP record is used as seed. (Only $a = 0.2$ is considered when the PUL record is used as seed.) Ensembles of 20 support motion arrays are simulated for each case of spatial variability.

It is of interest to investigate how spatial variability affects differences in the mean peak responses evaluated with consistent time-history and response spectrum analyses. For this reason, the case of uniform support excitations is also examined. For each bridge model, the input excitation in this case is the motion at a reference support from the ensemble of arrays simulated for $a = 0.2$. The reference supports are bent 3 for Penstock Bridge, bent 2 for South Ingram Slough Bridge, bent 2 for Big Rock Wash Bridge and bent 4 for Auburn Ravine Bridge.

The mean response spectra obtained by averaging 5% damped spectra for all simulations and all support points determine the respective input for the MSRS analysis. Averaging over all support motions is valid because under uniform soil conditions the response spectra at all support points should be the same. Response spectra values for damping ratios other than 5% are evaluated by adjusting the 5% damped spectral values according to Caltrans specifications (Caltrans SDC, 2004). The coherency function used to evaluate the MSRS correlation coefficients is the theoretical model in Eqn. 4.1. Konakli and Der Kiureghian (2012) have shown that estimates of the coherency function from ensembles of simulated arrays of motions are in good agreement with the target theoretical model. These coherency estimates are obtained after smoothing and averaging over the ensemble of arrays, since the non-smoothed coherency estimated from a single pair of motions exhibits erratic behavior. In the case of uniform excitations, the MSRS rule reduces to the square-root of the quadruple-sum term representing the dynamic component of the response, which has the same form as the well known CQC rule (Der Kiureghian, 1981), but with a more accurate approximation of the cross-modal correlation coefficients.

5. ASSESSMENT OF THE MSRS RULE BY COMPARISONS WITH RHA RESULTS

Estimates of mean peak responses evaluated with the MSRS formula given by Eqn. 2.3 are compared with the actual means of the temporal peaks obtained from RHA using the decomposition formula in Eqn. 2.2. For consistent comparisons, the same integration method is used for the evaluation of the *i*th modal time-history response, $s_{ki}(t)$, as the *i*th-mode spectral value, $D_k(\omega_i, \zeta_i)$. The RHA results have been validated through comparisons with time-history analysis with software OpenSees, which performs integration of the equations of motion in matrix form with Rayleigh damping.

The responses examined are pier drifts, which are quantities particularly important from a design viewpoint. On the basis of the "equal displacement" rule (Veletsos and Newmark, 1960), for sufficiently flexible structures, pier drifts obtained from linear analysis can be used to approximately evaluate nonlinear demands. Preliminary analysis has indicated that, for the pier drifts of the specific bridge models, considering the first 4 modes in the analysis is sufficient. For the four bridges, the results of the analyses are presented in Tables 5.1-5.4. For each ground motion random field, the tables list mean peak responses evaluated with the RHA and MSRS approaches, as well as the errors in the MSRS values if the RHA results are considered exact. These errors are given in parentheses next to the MSRS estimates. For each bridge and ground motion random field, mean values of the (algebraic) errors obtained by averaging over all piers are also listed. For a selected pier of each bridge and for the ground motion fields characterized by $a = 0.2$ (both seed records), Figure 5.1 shows the time histories of the drift responses for the 20 simulated support motion arrays. In each graph, the 20 time histories are plotted and compared with the MSRS estimates represented by the thicker horizontal lines. These graphs provide an illustration of the variability of the peak responses over the ensemble of realizations. Note that in this figure the MSRS estimates are practically identical to the exact RHA mean peak values for the South Ingram Slough Bridge and the Auburn Ravine Bridge with the PUL record as seed.

Considering the absolute values of the MSRS errors for individual pier drifts (listed in Tables 5.1-5.4), the maximum error observed under uniform support motions is 10.0% (HSP seed, Auburn Ravine Bridge, bent 2: pier 2), whereas under variable support motions this is 12.3% (PUL seed, Penstock Bridge, bent 4). Considering the absolute values of the average MSRS errors over all pier drifts of each bridge (listed in Tables 5.1-5.4), the maximum error observed under uniform support motions is 2.4% (HSP seed, Auburn Ravine Bridge), whereas under variable support motions this is 8.0% (HSP seed, $a = 0.4$, Auburn Ravine Bridge). In most cases, the errors are negative, i.e. the response spectrum approach underestimates the time-history response. Under uniform support motions, the mean (standard deviation) of the absolute values of the errors over all piers and bridges is 2.4% (2.6%) for HSP as seed and 3.3% (2.5%) for PUL as seed. Under variable support motions, the mean (standard deviation) of the absolute values of the errors over all piers and bridges is 3.5% (4.3%) for HSP and $a = 0.2$, 6.0% (4.3%) for HSP and $a = 0.4$, and 4.4% (3.6%) for PUL.

The MSRS method is intended for use in conjunction with smooth response spectra that represent broadband excitations and a smooth coherency function. In our analysis, jagged response spectra from relatively narrowband excitations were used. Furthermore, the smooth coherency function used for evaluation of the correlation coefficients in the MSRS analysis differs from the actual coherency values for pairs of simulated support motions, which can exhibit large fluctuations around the theoretical model. Considering these differences, the results of the MSRS analysis are found to be remarkably accurate. The errors tend to be larger under spatially varying motions compared to the case of uniform excitations. This is because the case of variable support motions employs additional assumptions regarding the coherency model explained above and involves additional approximations in representing the pseudo-static component of the response and its cross with the dynamic component.

6. CONCLUSIONS

The accuracy of the MSRS method in evaluating mean peak responses of bridges subjected to spatially varying ground motions was assessed through comparisons with respective results from consistent RHA. Considering absolute values of the MSRS errors, the mean and standard deviation over all responses examined (pier drifts of four bridge models) and non-uniform ground motion fields considered (three cases) were 4.6% and 3.7%, respectively. The maximum error observed was 12.3%, but in most cases, the errors were smaller than 10%. The good agreement between the two analysis approaches showed that the MSRS method is a reliable tool for response spectrum analysis under differential support excitations.

REFERENCES

Abrahamson, N. A., Schneider, J. F. and Stepp, J.C. (1991). Empirical spatial coherency functions for application to soil-structure interaction analyses. *Earthquake Spectra* **7**,1-28.

California Department of Transportation (2004). Caltrans Seismic Design Criteria (SDC).

Der Kiureghian, A. (1981). A response spectrum method for random vibration analysis of MDF systems. *Earthquake Engineering and Structural Dynamics* **9**,419-435.

Der Kiureghian, A. (1996). A coherency model for spatially varying ground motions. *Earthquake Engineering*

and Structural Dynamics **25**,99-111.
Der Kiureghian, A. and Neuenhofer, A. (1992). Response spectrum method for multiple-support seismic excitation. *Earthquake Engineering and Structural Dynamics* **21:7**,13-740.
Eurocode 8: Design of structures for earthquake Resistance-Part 2: Bridges (1998).
Harichandran, R. S. and Vanmarcke, E. H. (1986). Stochastic variation of earthquake ground motion in space and time. *Journal of Engineering Mechanics* **112**,154-174.
Kahan, M., Gibert, R.J. and Bard, P.Y. (1996). Influence of seismic waves spatial variability on bridges: a sensitivity analysis. *Earthquake Engineering and Structural Dynamics* **25**,795-814.
Konakli, K. and Der Kiureghian, A. (2011a). Extended MSRS rule for seismic analysis of bridges subjected to differential support motions. *Earthquake Engineering and Structural Dynamics* **40:12**,1315-1335.
Konakli, K. and Der Kiureghian, A. (2011b). Stochastic dynamic analysis of bridges subjected to spatially varying ground motions. *Report No. UCB/EERC-11/08*, Earthquake Engineering Research Center, University of California, Berkeley,
Konakli, K. and Der Kiureghian, A. (2012). Simulation of spatially varying ground motions including incoherence, wave-passage and differential site-response effects. *Earthquake Engineering and Structural Dynamics* **41:3**,495–513.
Loh, C.H. and Ku, B.D. (1995). An efficient analysis of structural response for multiple-support seismic excitations. *Engineering Structures* **17**,15-26.
Luco, J.E. and Wong, H.L. (1986). Response of a rigid foundation to a spatially random ground motion. *Earthquake Engineering and Structural Dynamics* **14**,891-908.
Veletsos, A.S. amd Newmark, N.M. (1960). Effect of inelastic behavior on the response of simple systems to earthquake motions. *Proceedings of the 2nd World Conference on Earthquake Engineering*, Japan, **2**,895-912.
Yu, R.F. and Zhou, X.Y. (2008). Response spectrum analysis for non-classically damped linear system with multiple-support excitations. *Bulletin of Earthquake Engineering* **6**,261-284.

Table 5.1. Penstock bridge: Mean peak pier drifts (in meters) from RHA and MSRS analyses and respective MSRS errors

seed: HSP						
location	uniform motions		variable motions, $a = 0.2$		variable motions, $a = 0.4$	
	RHA	MSRS (% error)	RHA	MSRS (% error)	RHA	MSRS (% error)
bent 2	0.322	0.322 (**0.0**)	0.294	0.289 (−**1.7**)	0.325	0.320 (−**1.5**)
bent 3	0.302	0.296 (−**2.0**)	0.281	0.271 (−**3.6**)	0.299	0.302 (**1.0**)
bent 4	0.241	0.230 (−**4.6**)	0.303	0.272 (−**10.2**)	0.295	0.273 (−**7.5**)
average		(−**2.2**)		(−**5.2**)		(−**2.7**)
seed: PUL						
location	uniform motions		variable motions, $a = 0.2$			
	RHA	MSRS (% error)	RHA	MSRS (% error)		
bent 2	0.468	0.466 (−**0.4**)	0.449	0.420 (−**6.5**)		
bent 3	0.434	0.430 (−**0.9**)	0.408	0.396 (−**2.9**)		
bent 4	0.353	0.334 (−**5.4**)	0.448	0.393 (−**12.3**)		
average		(−**2.2**)		(−**7.2**)		

Table 5.2. South Ingram Slough Bridge: Mean peak pier drifts (in meters) from RHA and MSRS analyses and respective MSRS errors

seed: HSP						
location	uniform motions		variable motions, $a = 0.2$		variable motions, $a = 0.4$	
	RHA	MSRS (% error)	RHA	MSRS (% error)	RHA	MSRS (% error)
bent 2: pier 1	0.217	0.217 (**0.0**)	0.207	0.206 (−**0.5**)	0.197	0.196 (−**0.5**)
bent 2: pier 2	0.217	0.217 (**0.0**)	0.207	0.206 (−**0.5**)	0.197	0.196 (−**0.5**)
average		(**0.0**)		(−**0.5**)		(−**0.5**)
seed: PUL						
location	uniform motions		variable motions, $a = 0.2$			
	RHA	MSRS (% error)	RHA	MSRS (% error)		
bent 2: pier 1	0.387	0.387 (**0.0**)	0.368	0.368 (**0.0**)		
bent 2: pier 2	0.387	0.387 (**0.0**)	0.368	0.368 (**0.0**)		
average		(**0.0**)		(**0.0**)		

Table 5.3. Big Rock Wash Bridge: Mean peak pier drifts (in meters) from RHA and MSRS analyses and respective MSRS errors

seed: HSP						
location	uniform motions		variable motions, $a = 0.2$		variable motions, $a = 0.4$	
	RHA	MSRS (% error)	RHA	MSRS (% error)	RHA	MSRS (% error)
bent 2: middle	0.063	0.061 (−**3.2**)	0.041	0.040 (−**2.4**)	0.045	0.042 (−**6.7**)
bent 2: side	0.063	0.061 (−**3.2**)	0.041	0.040 (−**2.4**)	0.045	0.042 (−**6.7**)
bent 3: middle	0.070	0.071 (**1.4**)	0.059	0.058 (−**1.7**)	0.062	0.059 (−**4.8**)
bent 3: side	0.070	0.071 (**1.4**)	0.059	0.058 (−**1.7**)	0.062	0.059 (−**4.8**)
average		(−**0.9**)		(−**2.1**)		(−**5.8**)
seed: PUL						
location	uniform motions		variable motions, $a = 0.2$			
	RHA	MSRS (% error)	RHA	MSRS (% error)		
bent 2: middle	0.114	0.111 (−**2.6**)	0.072	0.079 (**9.7**)		
bent 2: side	0.114	0.111 (−**2.6**)	0.072	0.079 (**9.7**)		
bent 3: middle	0.123	0.126 (**2.4**)	0.121	0.115 (−**5.0**)		
bent 3: side	0.123	0.126 (**2.4**)	0.121	0.115 (−**5.0**)		
average		(−**0.1**)		(**2.4**)		

Table 5.4. Auburn Ravine Bridge: Mean peak pier drifts (in meters) from RHA and MSRS analyses and respective MSRS errors

seed: HSP						
location	uniform motions		variable motions, $a = 0.2$		variable motions, $a = 0.4$	
	RHA	MSRS (% error)	RHA	MSRS (% error)	RHA	MSRS (% error)
bent 2: pier 1	0.041	0.038 (−**7.3**)	0.033	0.032 (−**3.0**)	0.033	0.033 (**0.0**)
bent 2: pier 2	0.040	0.036 (−**10.0**)	0.033	0.033 (**0.0**)	0.033	0.033 (**0.0**)
bent 3: pier 1	0.059	0.057 (−**3.4**)	0.030	0.029 (−**3.3**)	0.035	0.031 (−**11.4**)
bent 3: pier 2	0.057	0.055 (−**3.5**)	0.028	0.029 (**3.6**)	0.033	0.030 (−**9.1**)
bent 4: pier 1	0.074	0.073 (−**1.4**)	0.035	0.034 (−**2.9**)	0.042	0.037 (−**11.9**)
bent 4: pier 2	0.073	0.072 (−**1.4**)	0.034	0.033 (−**2.9**)	0.041	0.036 (−**12.2**)
bent 5: pier 1	0.081	0.081 (**0.0**)	0.047	0.045 (−**4.3**)	0.052	0.047 (−**9.6**)
bent 5: pier 2	0.081	0.081 (**0.0**)	0.045	0.043 (−**4.4**)	0.051	0.046 (−**9.8**)
bent 6: pier 1	0.077	0.078 (**1.3**)	0.061	0.056 (−**8.2**)	0.062	0.057 (−**8.1**)
bent 6: pier 2	0.078	0.079 (**1.3**)	0.060	0.055 (−**8.3**)	0.061	0.056 (−**8.2**)
average		(−**2.4**)		(−**3.4**)		(−**8.0**)
seed: PUL						
location	uniform motions		variable motions, $a = 0.2$			
	RHA	MSRS (% error)	RHA	MSRS (% error)		
bent 2: pier 1	0.080	0.077 (−**3.8**)	0.082	0.087 (**6.1**)		
bent 2: pier 2	0.079	0.076 (−**3.8**)	0.083	0.089 (**7.2**)		
bent 3: pier 1	0.107	0.099 (−**7.5**)	0.069	0.068 (−**1.4**)		
bent 3: pier 2	0.104	0.097 (−**6.7**)	0.069	0.069 (**0.0**)		
bent 4: pier 1	0.129	0.122 (−**5.4**)	0.057	0.057 (**0.0**)		
bent 4: pier 2	0.127	0.120 (−**5.5**)	0.057	0.056 (−**1.8**)		
bent 5: pier 1	0.131	0.131 (**0.0**)	0.070	0.072 (**2.9**)		
bent 5: pier 2	0.132	0.130 (−**1.5**)	0.066	0.068 (**3.0**)		
bent 6: pier 1	0.118	0.125 (**5.9**)	0.116	0.109 (−**6.0**)		
bent 6: pier 2	0.119	0.126 (**5.9**)	0.109	0.104 (−**4.6**)		
average		(−**2.2**)		(**0.5**)		

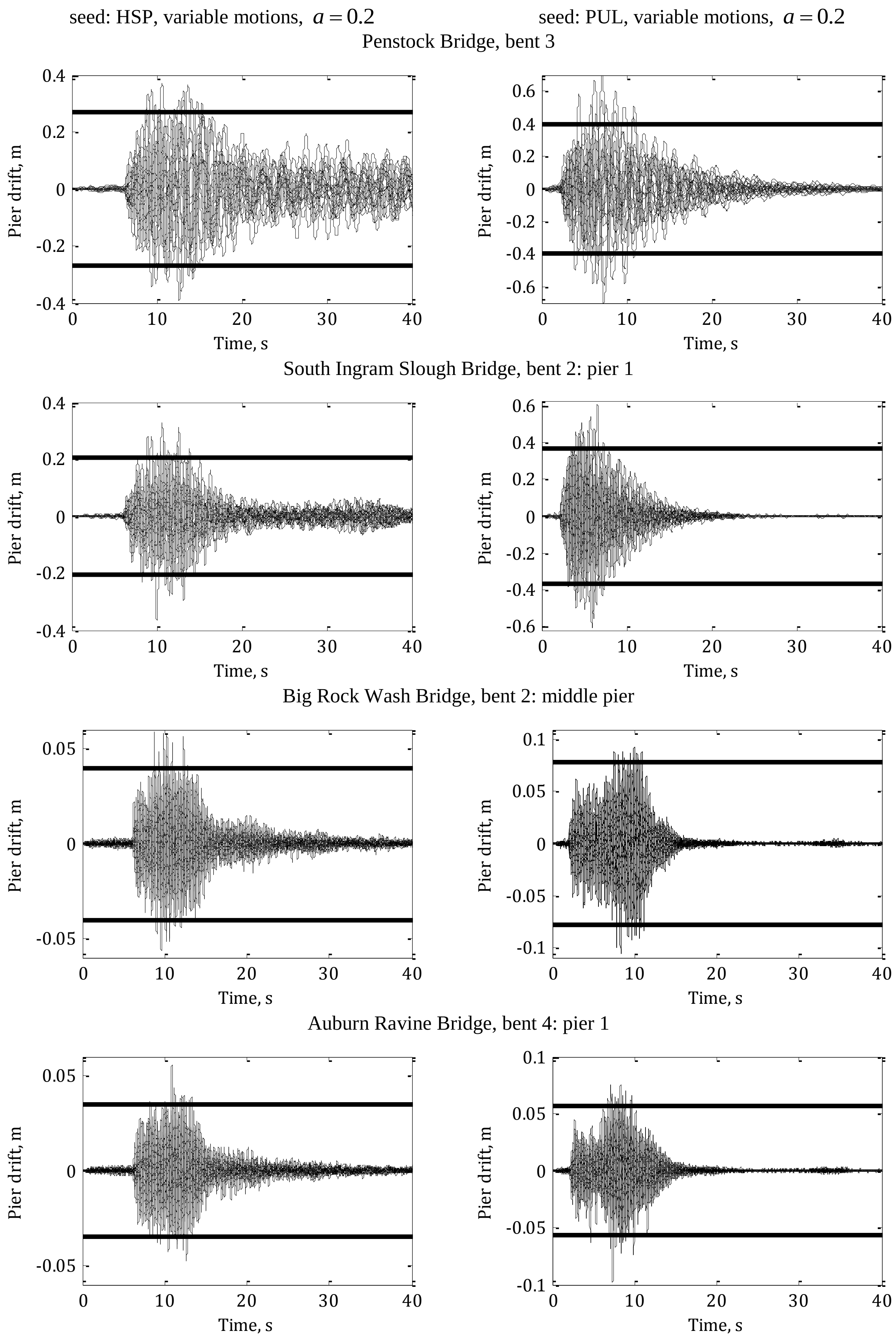

Figure 5.1. RHA and MSRS pier drift responses